Toxicology Letters 218 (2013) 61–69

Contents lists available at SciVerse ScienceDirect

Toxicology Letters

journal homepage: www.elsevier.com/locate/toxlet

Phosphoproteome analysis reveals an important role for glycogen synthase kinase-3 in perfluorododecanoic acid-induced rat liver toxicity

Hongxia Zhang[a,1], Junjie Hou[b,1], Ruina Cui[a], Xuejiang Guo[c], Zhimin Shi[a], Fuquan Yang[b], Jiayin Dai[a,*]

[a] Key Laboratory of Animal Ecology and Conservation Biology, Institute of Zoology, Chinese Academy of Sciences, Beijing 100101, China
[b] Laboratory of Proteomics, Institute of Biophysics, Chinese Academy of Sciences, Beijing, China
[c] State Key Laboratory of Reproductive Medicine, Nanjing Medical University, Nanjing, China

HIGHLIGHTS

- A total of 1443 unique phosphopeptides from 769 phosphoproteins were identified.
- A total of 143 unique phosphorylation sites were considered to be novel.
- Chronic PFDoA exposure inhibited insulin signal pathway.
- Inhibition of GSK3 might contribute to increase lipid levels in PFDoA treated liver.

GRAPHICAL ABSTRACT

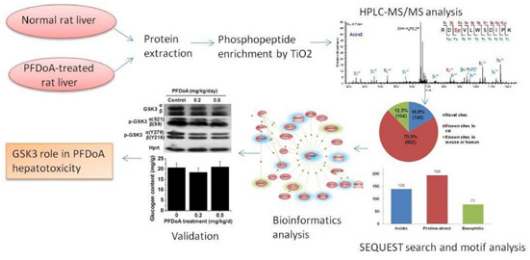

ARTICLE INFO

Article history:
Received 6 December 2012
Received in revised form 11 January 2013
Accepted 16 January 2013
Available online 24 January 2013

Keywords:
Perfluorododecanoic acid (PFDoA)
Phosphoproteome
Liver
GSK3β

ABSTRACT

Perfluorododecanoic acid (PFDoA) is a member of the perfluoroalkyl acid (PFAA) family and has broad applications and a wide distribution in the environment. Here, we used TiO_2-based phosphopeptide enrichment coupled with LC–MS/MS analysis to identify phosphopeptides in rat livers that were influenced by PFDoA treatment. We identified a total of 1443 unique phosphopeptides from among 769 phosphoproteins identified in normal and PFDoA-treated rat livers, 849 unique phosphorylation sites were also identified. Of these sites, 143 were considered to be novel phosphorylation sites. Many phosphoproteins were found to be associated with hepatic injuries and diseases, such as hepatotoxicity, regeneration, fatty liver, neoplasms and carcinoma. Furthermore, 25 of the identified phosphoproteins were found to be related to glycogen synthase kinase-3 (GSK3), either directly or indirectly. Western blot and qPCR results suggested that chronic PFDoA exposure inhibited insulin signal pathways and that inhibition of GSK3 might contribute to the observed increases of lipid levels in the liver.

1. Introduction

Perfluoroalkyl acids (PFAAs) including perfluorooctanoic acid (PFOA, C8), perfluorooctansulfonate (PFOS, C8) and perfluorododecanoic acid (PFDoA, C12) are a class of highly stable compounds used widely in commercial and industrial applications as surfactants, lubricants, paints, polishes, paper and textile coatings, food packaging and fire-retardant foams (Kissa, 2001). They have strong C—F bonds which enable them to resist hydrolysis, photolysis, biodegradation and metabolism, leading to their wide global distribution (Kissa, 2001; Pan et al., 2011; Zhang et al., 2010), bioaccumulation (Houde et al., 2006; Martin et al., 2004; Pan et al., 2011) and various toxicities (Lau et al., 2004, 2007). Several studies addressing PFAAs with C7—C10 indicated that PFAAs with longer carbon chains were eliminated more slowly and thus, were more bioaccumulative and toxic than those with a shorter carbon chain (Kudo et al., 2006; Ohmori et al., 2003). Accordingly, PFDoA, with twelve carbon atoms, is likely to be more hazardous

Abbreviations: PFDoA, perfluorododecanoic acid; GSK3, glycogen synthase kinase-3; SREBP1c, sterol regulatory element binding protein 1c; TG, triglyceride; TC, total cholesterol.

* Corresponding author. Tel.: +86 0 10 64807085; fax: +86 0 10 64807099.
E-mail address: daijy@ioz.ac.cn (J. Dai).

[1] These authors contributed equally to this article.

0378-4274/$ – see front matter © 2013 Elsevier Ireland Ltd. All rights reserved.
http://dx.doi.org/10.1016/j.toxlet.2013.01.012

to the environment and human health than PFOA and PFOS. PFDoA has been identified in water, soil, wildlife and humans (Guruge et al., 2005; Liu et al., 2011; Olsen et al., 2011), but it has not been subjected to toxicological analyses despite the high accumulated environmental concentrations detected. For example, the highest concentration of PFDoA observed in beluga livers from Arctic locations was 9.89 ng/g (Reiner et al., 2011). Unlike most other persistent organic pollutants (POPs), which accumulate in lipid-rich tissues, PFAAs can bind to blood and liver proteins and accumulate mainly in the liver, kidneys and bile secretions (Jones et al., 2003). PFAAs increase the liver-to-body weight ratio, lipid levels, hepatocellular hypertrophy, and peroxisome proliferation and induce liver tumors in hepatocytes in laboratory animals (Kennedy et al., 2004). Although many studies have attempted to explore the mechanisms underlying PFAA hepatotoxicity (Rosen et al., 2010; Shi et al., 2009; Wei et al., 2008), few studies have addressed the effect of PFAAs on post-translational regulation.

Reversible protein phosphorylation is the most common type of PTM and is involved in almost all cellular and developmental processes. This reversible type of phosphorylation is mediated by the opposite actions of large families of protein kinases and phosphatases (Zolnierowicz and Bollen, 2000). Many diseases such as cancer, auto-immune diseases, metabolic disorders and pathogenic infections are associated with protein kinase-mediated signaling pathways (Gatzka and Walsh, 2007; Hanahan and Weinberg, 2000; Taniguchi et al., 2006). Therefore, large-scale analysis of differentially regulated phosphorylation events associated with different biological conditions can be used to identify and understand complex signaling networks. Mass spectrometry (MS) has become a powerful tool for the global identification of phosphorylated proteins and the characterization of phosphorylation sites due to its high level of sensitivity and accuracy. In addition, various phosphopeptide enrichment methods such as the use of titanium dioxide (TiO_2) (Larsen et al., 2005), IMAC (Ficarro et al., 2002), strong cation exchange (SCX) chromatography (Beausoleil et al., 2004), and other methods (Kweon and Hakansson, 2006; Rush et al., 2005), have been developed recently and applied to obtain large phosphorylation profiles in many biological systems. However, due to the complexity of the tissue samples, the selection of ions for MS/MS fragmentation varied between analyses. This led to less reproducibility of the phosphopeptides identified in two independent analyses for a given sample mixture (Moser and White, 2006). Thus, the label-free quantification of protein phosphorylation in tissue extracts remained challenging and lacked standard methods.

In this study, we performed a phosphoproteomic analysis of rat liver both with and without PFDoA treatment employing TiO_2-based phosphopeptide enrichment followed by LC–MS/MS analysis. We did not quantify the change of phosphorylation level of certain proteins in different PFDoA treatments through counting phosphopeptide numbers in this study. Moreover, we performed several different bioinformatics analyses to find the possible proteins and biological processes affected by PFDoA. Then, qPCR and western blot analysis was used to verify the transcriptional regulation and phosphorylation levels of a number of signaling molecules in response to PFDoA. Our work provides further insight into the molecular mechanisms underlying PFDoA hepatotoxicity and the possibility of discovering new biomarkers based on exposure to PFDoA.

2. Materials and methods

2.1. Animal treatment

Male Sprague-Dawley rats (230–240 g) were obtained from Weitong Lihua Experimentary Animal Central (Beijing, China). After one week of adaptation, the rats were separated into three groups. The treatment rats were given doses of 0.2 and 0.5 mg of PFDoA (Sigma–Aldrich, dissolved in 0.2% Tween-20) per kg of body weight/d *via* oral gavage for 110 consecutive days. Control animals were fed with only 0.2% Tween-20 (vehicle) in a similar manner. At the end of the experiment, six rats from each group were euthanized by decapitation. The liver was immediately removed, washed with PBS and divided into small aliquots. One portion was fixed in 10% neutral buffered formalin for histological examination, while the others were flash frozen in liquid nitrogen and stored at −80 °C.

2.2. Sample preparation, in-solution tryptic digestion and phosphopeptide enrichment

The total protein was extracted from the rat liver samples and the details given in supplemental data. Tryptic digestion was carried out according to a previously described method with some modifications (Dai et al., 2007). A phosphopeptide enrichment procedure described previously (Wu et al., 2007) was used in this study with some modification.

2.3. LC–MS/MS analysis on LTQ-Orbitrap

All phosphopeptides were analyzed using a nanoscale HPLC–MS system. A Surveyor liquid chromatography system was coupled online to an LTQ-Orbitrap mass spectrometer (Thermo Fisher Scientific, San Jose, CA) equipped with a nanoelectrospray interface operated in positive ion mode. Separation was performed on a C18 reverse phase column (75 μm × 15 cm, Column Technology Inc., CA). The flow rate was 140 μL/min prior to splitting and 200 nL/min after splitting. Peptides were eluted using a linear gradient with the percentage mobile phase B (0.1% FA in ACN) increasing from 2 to 35% in 120 min. The spray voltage was set to 1.85 kV, and the temperature of the heated capillary was 160 °C. The normalized collision energy was 35.0. The mass spectrometer was set to perform a full MS scan, followed by ten MS/MS scans on the ten most intense ions from the MS spectrum, with the following Dynamic Exclusion settings: repeat count 2, repeat duration 0.5 min, and exclusion duration at 90 s. The resolving power of the Orbitrap mass analyzer was set at 100,000 ($m/\Delta m$ 50% at m/z 400) for the precursor ion scans.

2.4. Database searching, data filtering and site localization

The derived mass spectrometry datasets were converted to generic format (*.dta) files using Bioworks 3.2. These files were then searched against the real and reverse IPI rat protein sequence database (version 3.28) using the SEQUEST searching program. Trypsin was designated as the protease, with two missed cleavage sites being allowed. The search parameters included: carboxyamidomethylation modification of cysteine as a fixed modification, phosphorylationon serine, threonine, and tyrosine as dynamic modifications and oxidation on methionine as a variable modification. Up to six phosphorylation sites were allowed per peptide. Previously published filter parameters were set for phosphopeptide identification (Wu et al., 2007), with a ΔCn score of at least 0.1 required, regardless of charge state, and a false discovery rate (FDR) of ≤1%. The FDR was calculated based on the following formula: % fal = $n_{rev}/(n_{rev} + n_{real})$, where n_{rev} is the number of peptide hits matched to a "reverse" protein and n_{real} is the number of peptide hits matched to a "real" protein. In addition, every spectrum of the phosphopeptides was manually checked to ensure that the fragment ion peaks have a high signal-to-noise ratio. Precursor ion mass tolerances were 10 ppm and a fragment ion mass tolerance was 0.8 Da. The two mass spectrometry datasets for the same treatment were combined for future phosphoprotein group identification.

For phosphorylation site localization, each SEQUEST-identified phosphorylation site from the peptides in Table S1 was subjected to analysis using ArNone software (Jiang et al., 2010). Sites with Ascore values above 19 were considered to be localized with near certainty, while those with scores between 13 and 19 were considered to be localized with high certainty. Unique novel sites were confirmed by searching the combined phosphorylation sites (Ascore value above 19) in all groups inside the rat database on the UniProt (http://www.uniprot.org) and PhosphoSite (http://www.phosphosite.org) website and manually excluding sites homologous to both humans and mice.

For protein identification, we used the IPI database, which offers complete non-redundant datasets built from the Swiss-Prot, TrEMBL, Ensembl and RefSeq databases. A protein group was removed if all identified peptides assigned to that protein group were also assigned to another protein group. To extract a single protein member from a protein group, we chose the protein with the highest sequence coverage.

2.5. Data analysis

Specific motifs were obtained from the combined datasets for all treatments using the Motif-x algorithm (http://motif-x.med.harvard.edu) (Schwartz and Gygi, 2005). All single phosphorylation and extendible sites (non-N/C-terminal peptides) with an Ascore ≥ 19 were used for motif analysis. NetworKIN-2.0 (Linding et al., 2007) was used to predict probable kinase families for the identified phosphorylation sites. Because *Rattus norvegicus* was not included in the NetworKIN database, human taxonomy was chosen as an alternative, as it is generally assumed that kinase substrates are highly conserved between humans and rats. Kinase–substrate

Table 1
Summary of characteristics of phosphorylated proteins in rat liver.

	PFDoA (mg/kg/day)		
	0	0.2	0.5
Total peptides	2749	1316	1931
Unique peptides	959	577	818
Protein groups	561	363	479

relationships with a NetworKIN score > 1.0 and a String score > 0.6 were regarded as significant.

All gene ontology data for the phosphoproteins were obtained by searching the Gene Ontology database (http://www.geneontology.org/). Further analysis was performed using the GOstat program (http://gostat.wehi.edu.au/) to sort the GO annotations to find functional annotations that were highly represented in the data. Analyses of diseases associated with the identified phosphoproteins and the interactions among these proteins in the control and PFDoA-treated groups were performed using Pathway StudioTM (v7.0) software (Ariadne Genomics, Inc. Rockville, MD).

2.6. Western blotting and phosphopeptide validation

Western blot analysis was performed according to the standard procedure described previously (Zhang et al., 2011). The primary antibodies used were rabbit polyclonal antibodies for rat glycogen synthase kinase (GSK3β), GSK3β (pT216), GSK3β (pS9), protein kinase 1 (PDK1), PDK1 (pS241), Akt (Signalway Antibody), insulin receptor substrates (IRS1, pS1101), IRS1 (pS302), PI3K (Abcam) and Akt (pS473) (Cell Signaling Technology).

Two phosphopeptides (RDSpVLWSDIPK and AGSpDTELAAPK) were synthesized with a purity > 98% (Scilight Biotechnology, Beijing, China) and analyzed by LTQ-Orbitrap mass spectrometry as described above. The MS/MS spectra of synthesized peptides were compared with those of the identified peptides.

2.7. Determination of triglyceride (TG), total cholesterol (TC) and glycogen content in the liver

Liver lipids were extracted using a mixture of chloroform/methanol (2:1, v/v). Liver TG and TC were analyzed using commercial kits according to the manufacturer's recommendations (Biosino Bio-technology and Science Inc., Beijing, China). Liver homogenates (10% in 0.9% NaCl) were employed to assay glycogen levels using kits according to the user's manual (Nanjing Jiancheng Bioengineering Institute, Nanjing, China). In addition, a portion of each liver sample which was fixed in 10% neutral buffered formalin was embedded in paraffin, cut and stained with periodic acid-Schiff (PAS) staining. Glycogen levels were observed under a light microscope.

2.8. Quantitative real-time PCR analysis

Total RNA extraction and qPCR analysis was performed as described previously (Zhang et al., 2011). The rat-specific primers were given in supplemental data for specific genes: sterol regulatory element binding protein 1c (SREBP-1c), fatty acid synthase (FASn), stearoyl-CoA desaturase 1 (SCD1), and fatty acid translocase (CD36). Hprt1 was chosen as an internal control.

3. Results and discussion

3.1. Phosphoproteomic analysis of rat liver following PFDoA treatment via LC–MS/MS

To perform a phosphoproteomic analysis of rat livers that were or were not subjected to PFDoA treatment, rats were exposed to three different levels of PFDoA (0, 0.2, and 0.5 mg/kg/d) for 110 days. Liver extracts of equal quality from six rats in each group were pooled to yield a single liver protein sample mixture and digested with trypsin. Phosphopeptides were further enriched with TiO_2 and analyzed *via* LC–MS/MS analysis. Two independent analyses of each of the three treatments were performed, and the resultant raw data (for each treatment) were combined for further protein group assignment and data analysis (Table S1). A total of 959, 577 and 818 unique phosphopeptides from 561, 363 and 479 phosphoproteins were identified with a FDR < 1% following the 0, 0.2, and 0.5 mg/kg/d PFDoA treatments, respectively (Table 1, Fig. S1 and Table S2). After combining all of the results from all independent experiments, the percentages of peptides presenting single, double and triple phosphorylated sites were 94.6%, 4.3% and 1.2%, respectively (Fig. 1A).

Two of these identified phosphopeptides, RDSpVLWSDIPK from peroxisomal acyl-CoA oxidase 3 (Acox3) and AGSpDTELAAPK from FASn, were obtained as synthetic peptides. The MS2 spectra of these phosphopeptides obtained from TiO_2-enriched liver extracts were almost identical to the MS2 spectra of synthesized peptides (Fig. S2), indicating accurate identification was achieved.

The ArMone software suite was then used to calculate the Ascore value of each phosphorylated site; the Ascore value distribution for all of the phosphorylation sites revealed that 61.1% of the sites had Ascore values of at least 19, indicating near certainty, and 8.2% of phosphorylation sites had Ascore values between 13 and 19, indicating high certainty (Fig. 1B). A total of 849 unique phosphorylation sites with an Ascore of greater than 19 were detected in this study (Table S3). By analyzing the phosphorylated amino acids, the distribution of all unique phosphorylation sites was found to consist of 85.8% phosphoserines, 12.1% phosphothreonines and 2.1% phosphotyrosines (Fig. 1C), which is consistent with the pSer:pThr:pTyr ratios reported by Olsen (86.4:11.8:1.8) and Nagano (86:12:2) in HeLa cells (Nagano et al., 2009; Olsen et al., 2006). Furthermore, retrieval of phosphorylation site (Ascore ≥ 19) information from the UniProt and PhosphoSite rat databases indicated 143 sites were considered to be novel phosphorylation sites for 124 phosphoproteins; this was accomplished by manually checking and excluding sites homologous to both humans and mice (Fig. 1D and Table S3).

Because the liver is the main organ that regulates metabolism, it is not surprising that some of these 124 phosphoproteins were related to metabolism (Table 2). For example, several enzymes, such as FASn (Ser2191), hydroxymethylglutaryl-CoA synthase (HMGCS; Ser477), very long-chain acyl-CoA synthetase (SLC27a2; Ser209), and peroxisomal bifunctional enzyme (EHHADH; Ser705 and Thr27), that play important roles in lipid metabolism have been reported to be phosphoproteins, although the relationships between their activities and the observed phosphorylation events are currently unknown. The activities of several phosphoproteins associated with glucose metabolism, such as glycogen synthase (GYS2; Ser627) and Akt2 (Ser461), are known to be regulated by dephosphorylation or phosphorylation of specific sites, which have been previous characterized (Hers et al., 2011; Ros et al., 2009). In addition, this is the first study to identify phosphorylation sites in certain proteins involved in xenobiotic metabolism, including cytochrome P450 family members (Cyp2a1, Cyp2S1; Ser130 in Cyp2a1, Ser84 in Cyp2S1, respectively) and epoxide hydrolase 1 (EPHX1; Ser38 and Ser41). The novel phosphorylation sites identified here not only enrich the phosphoprotein database but will also aid future research addressing functional proteins.

3.2. Motif analysis and kinase prediction

The Motif-X algorithm was used to extract significant phosphorylation sequence motifs from our dataset, and NetworKIN (version 2.0) was used to reveal the kinase–substrate relationships. A total of 8 serine motifs and 1 threonine motif was found in this study (Table S4). These motifs can be divided into 3 general classes: acidic motifs, such as [S#D/ExE], [S#xD/E] and [S#xxD], which are recognized as substrates of casein kinase II (CK2); basophilic motifs, such as [RRxS#] and [RxxS#], which are specific recognition sites for PKA/PKC (Amanchy et al., 2007); and proline-directed phosphorylation motifs [T/S#P], which are substrates of many kinases, such as cyclin-dependent kinase 1 (CDK1) and members of the MAPK group (p38 and JNK). Similar to another study (Villen et al., 2007), we identified more proline-directed and acidic motifs than basic motifs. Proline-directed phosphorylation motifs were found

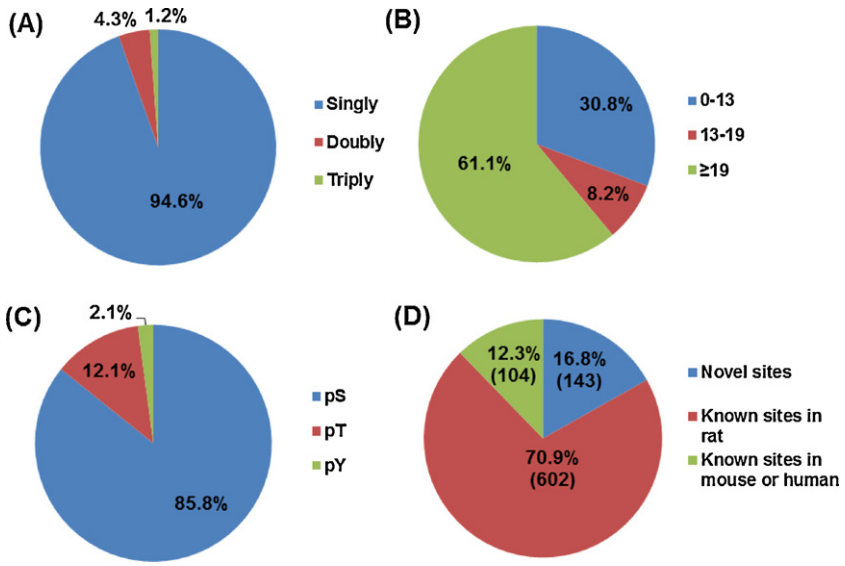

Fig. 1. General description of the phosphoproteomic data obtained in this study. (A) Distribution of single, double and triple phosphorylated peptides. (B) Ascore value distribution for all identified phosphorylation sites. (C) Frequency of phosphoserine (pS), phosphothreonine (pT) and phosphotyrosine (pY) residues with an Ascore greater than 19. (D) Number of novel and known phosphorylated sites among all peptides detected (Ascore > 19).

nearly 200 times in total and were the most abundant motifs detected (Table S4), while acidic motifs were detected 139 times (Fig. 2A). Interestingly, the percentage of acidic motif proteins, such as CK2 substrates, was the highest among the detected motifs, while proline-directed kinases were the most frequently observed phosphoserine/threonine kinases, including members of the p38 group, cyclin-dependent kinase 2 (CDK2) and the JNK group (Fig. 2B). These results were consistent with the motif distribution derived from Motif-X analysis and suggested that s/tP kinases tend to be more active than s-D/E kinases in the rat liver.

Table 2
Partial phosphoproteins related to metabolism with novel phosphorylation sites detected in this study.

Protein description	Gene symbol	IPI accession	Phosphorylation sequence	Site
Lipid metabolism[a]				
Fatty acid synthase	Fasn	IPI00200661.1	AGS#DTELAAPK	S2191
Very long-chain acyl-CoA synthetase	Slc27a2	IPI00205417.5	VDGVSADPIPES#WR	S209
Hydroxymethylglutaryl-CoA synthase, mitochondrial precursor	Hmgcs2	IPI00210444.5	VNFS#PPGDTSNLFPGTWYLER	S477
5′-AMP-activated protein kinase subunit beta-1	Prkab1	IPI00231108.5	SQNNFVAILDLPEGEHQY#K	Y125
Peroxisomal bifunctional enzyme	Ehhadh	IPI00232011.9	LVAQGS#PPLK	S705
Peroxisomal bifunctional enzyme	Ehhadh	IPI00232011.9	LCNPPVNAVSPT#VIR	T27
NOL1/NOP2/Sun domain family, member 2	Nsun2_predicted	IPI00364693.3	FQQPPQPEGEEDGS#DGSR	S48
Amino acid metabolism				
Similar to glutathione S-transferase zeta 1 isoform 2	LOC681913	IPI00193221.2	VDLS#PYPTISHINK	S139
Cystathionine gamma-lyase	Cth	IPI00194550.5	QDS#PGQSSGFVYSR	S50
Dihydropyrimidinase	Dpys	IPI00205906.2	DQTCT#PIPVK	T484
Arginase-1	Arg1	IPI00327518.4	DHGDLAFVDVPNDS#PFQIVK	S74
Carbohydrate metabolism				
RAC-beta serine/threonine-protein kinase	Akt2	IPI00212846.3	YDSLGS#LELDQR	S461
Glycogen synthase	Gys2	IPI00324172.2	FHLEPTS#PPTTDGFK	S627
Similar to aldehyde dehydrogenase 1 family, member L2	Aldh1l2_predicted	IPI00361193.5	T#PQPEEGATYEGIQK	T213
Xenobiotic metabolism				
Cytochrome P450 2A1	Cyp2a1	IPI00196696.6	RLS#IATLR	S130
Epoxide hydrolase 1	Ephx1	IPI00209690.1	DKEETLPLGDGWWGPGS#KPSAK	S38
Epoxide hydrolase 1	Ephx1	IPI00209690.1	DKEETLPLGDGWWGPGSKPS#AK	S41
Glutathione S-transferase alpha-1	Gsta2;Yc2;Gsta3	IPI00231638.6	ISS#LPNVK	S190
Glutathione S-transferase Mu 1	Gstm1	IPI00231639.7	YLS#TPIFSK	S205
Cytochrome P450 2C11	Cyp2c	IPI00327781.1	RFS#IMTLR	S127
Cytochrome P450 2C11	Cyp2c	IPI00327781.1	ADS#LSSHL	S495
Cytochrome P450 2C11	Cyp2c	IPI00327781.1	ADSLSS#HL	S498
Cyp2s1 protein-like	Cyp2s1	IPI00734626.2	LLISELS#R	S84
Steriod metabolism				
Similar to RIKEN cDNA 4632417N05	Sdr42e1	IPI00768842.1	MGPVVLSLSRMDS#PR	S13
3-alpha-hydroxysteroid dehydrogenase	Akr1c9	IPI00211100.1	S#PVLLDDPVLCAIAK	S232
Energy metabolism				
Similar to type V P-type ATPase isoform 4	RGD1306927_predicted	IPI00362098.4	NESVSALS#ASPNVPEK	S1019

[a] The identified phosphorproteins are grouped according to their functions.

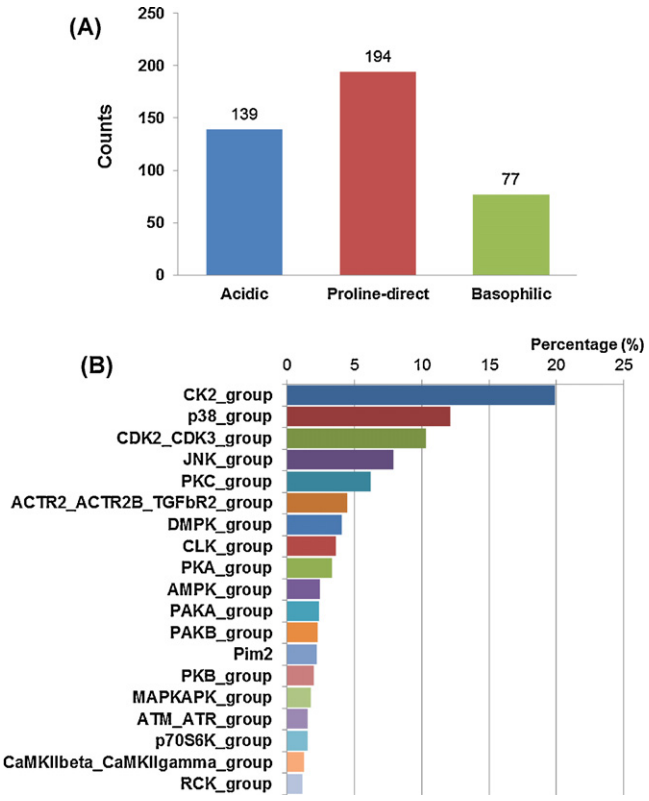

Fig. 2. Motif-X analysis and kinase prediction for all phosphorylated proteins identified in the rat livers. (A) Frequency of acidic, basic and proline-directed residues extracted in total. (B) Protein kinase analysis for all phosphorylated sites using NetworKin 2.0. The number of peptides phosphorylated by each kinase was divided by the total number of peptides phosphorylated by all of the kinases in one group to generate a percentage for each kinase.

3.3. GO analysis of phosphoproteins

For the determination of the types of phosphoproteins identified in the liver of normal and PFDoA-treated rats, GO analysis provided the functional annotations (including molecular function, cellular localization and biological process) of the phosphoproteins. Twenty categories which were highly represented were shown in Fig. S3. Overall, 460 of 561, 302 of 363 and 393 of 479 phosphoproteins were annotated in the 0, 0.2 and 0.5 mg/kg/d PFDoA treatment groups, respectively. Based on GOstart analysis, over half of the proteins (57.9%, 56.2% and 60.5%) were found to be related to protein binding in the three groups. Two other molecular functions attributed to more than 10% of the proteins in each group were nucleotide binding and ATP binding (Fig. S3A). In addition, the majority of the phosphoproteins identified in rat liver were found to be localized in the cytoplasm (~38%) and nucleus (~30%) (Fig. S3B). There was no obvious difference in the percentage of each function and location category between the PFDoA-treated and control groups. Phosphoproteins were involved in biological processes such as drug responses, amino acid phosphorylation, oxidation–reduction, metabolic processes, signal transduction and apoptosis. We compared the annotations of each phosphoproteome set obtained from the different groups with or without PFDoA treatment. Interestingly, compared to the control, the percentages of phosphoproteins in some annotation groups such as response to drugs, apoptosis signaling, oxidation–reduction, and cellular response to insulin stimulus increased in the PFDoA-treated groups. Previous studies have indicated that PFNA leads to cell apoptosis in the rat testis and thymus (Fang et al., 2009; Feng et al., 2009). Phosphorylation status of these proteins in different PFDoA treatments would provide a new horizon for studying the mechanism of PFDoA toxicity.

3.4. Signaling pathway analysis

To gain a better understanding of these phosphoproteins, detailed analyses of the interaction relationships among these proteins related to various diseases were performed using Pathway Studio software *via* the ResNet database. A total of 561 and 583 phosphoproteins in control and combined PFDoA-treated groups were subjected to analysis. Many phosphoproteins were found to be associated with hepatic injuries and diseases, such as liver toxicity, regeneration, fatty liver, neoplasms and carcinoma (Fig. 3A). For example, 21 proteins were related to liver toxicity, including heat shock proteins (HSPB1, HSP90AA1 and HSPD1), superoxide dismutase 1 (SOD) and glutathione peroxidase 1 (GPX1), which plays a significant role in oxidative stress reactions. Obvious spotty necrosis and steatosis as well as significant increases in the mRNA levels of HSPD1 and HSPB1 (1.36 fold and 3.53 fold) were observed in rat livers after 0.2 mg/kg/d PFDoA treatment for 110 days (Ding et al., 2009). In addition, SOD and GPX1 activity in the livers of rats and fish was found to be induced by acute PFAA exposure in previous studies (Liu et al., 2008; Zhang et al., 2008). To determine whether the phosphorylation of these proteins contributes to their functional alteration following PFAA exposure, further investigation will be necessary.

The results of the interaction relationship analyses showed that 25 of the phosphoproteins were regulated by phosphorylation of glycogen synthase kinase 3 (GSK3) either directly or indirectly (Fig. 3B). These proteins included IRS1, PDK1, protein kinase C, SREBP1, GYS2, and so on. GSK3 is a multifunctional serine/threonine (Ser/Thr) kinase that was first identified based on its ability to phosphorylate and inactivate glycogen synthase. It exists as two isoforms: GSK3α (51 kDa) and GSK3β (46 kDa), which are highly homologous (approximately 85% protein sequence similarity) (Woodgett, 1990). GSK3 activity is regulated by the phosphorylation of both serine and tyrosine residues. Phosphorylation of Ser21 in GSK3α and Ser9 in GSK3β decreases their activity, whereas an increase in activity is observed when Tyr279 in GSK3α and Tyr216 in GSK3β are phosphorylated (Frame et al., 2001; Hughes et al., 1993; Stambolic and Woodgett, 1994).

Therefore, we further investigated the role of GSK3 in the hepatotoxicity of PFDoA. Despite the fact that Tyr216 was the only GSK3β phosphorylation site (and Tyr279 was the GSK3α site) identified in the 0.5 mg PFDoA/kg/d group, both GSK3α/β protein levels and phosphorylation (Tyr279/216 and Ser21/9) could be detected. The results showed that the protein and phosphorylation levels of GSK3α/β in rat livers were both decreased following the PFDoA treatments (Fig. 4A), which indicated that sub-chronic exposure to PFDoA could inhibit GSK3α/β activity in rat livers *via* decreasing the GSK3 protein levels.

GSK3 is constitutively active and is significantly deactivated by insulin signaling through the sequential activation of IRS1, PI3K, and Akt to phosphorylate specific serine residues in the enzyme; as a result, an increase in glycogen synthase activity stimulates glycogen synthesis (Cross et al., 1995). Thus, the levels of glycogen in the liver and the expression levels of proteins upstream of GSK3 were measured. The results showed that liver glycogen levels did not change following PFDoA exposure for 110 days (Figs. S4A and S4B), indicating that PFDoA treatment did not increase the glycogen synthesis *via* GSK3 inhibition to increase glycogen synthase activity as a consequence. However, the phosphorylation levels of IRS1 (Ser1101 and Ser302), PDK1 (Ser241), and Akt (Ser473) and the protein levels of PI3K were all clearly down-regulated by PFDoA exposure (Fig. 4B), which suggested inhibition of PI3K, PDK1 and Akt activities. This suggests that inhibition of GSK3 activity by

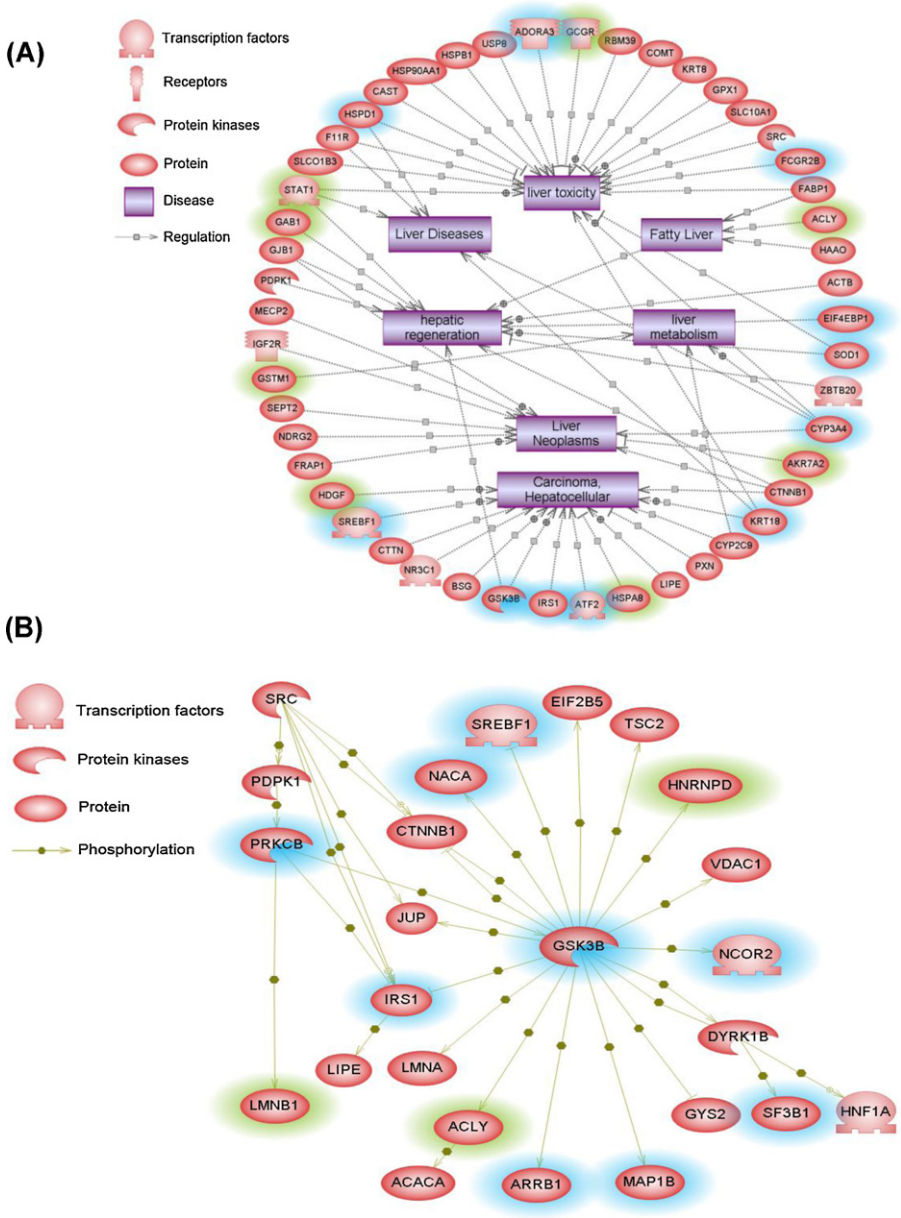

Fig. 3. Analysis of the regulatory network of all of the phosphorylated proteins identified in rat liver. The pathway analysis was performed using Pathway Studio (v 7.0) software. (A) The network of phosphoproteins that are related to diseases. (B) The network of proteins that are related to glycogen synthase kinase-3 beta (GSK-3β). The green shadow represents a protein only identified in the normal group. The blue shadow represents a protein only identified in the PFDoA-treated group. Table S5 provides a list of the abbreviations used in the figure. (For interpretation of the references to color in this figure legend, the reader is referred to the web version of the article.)

PFDoA is not dependent on the PI3K/PDK1/Akt pathway. In addition, we further detected the protein levels of GSK3, PDK1 and Akt and found that all the protein levels decreased in PFDoA treatments. Thus, we speculated that chronic PFDoA exposure could inhibit the insulin signal pathway by inhibiting the protein synthesis of related proteins. GSK3 has also been reported to down-regulate the transcriptional activity of ADD1/SREBP1c (Kim et al., 2004), a transcription factor that has been shown to inhibit the PI3K/Akt pathway, and phosphorylate IRS1 on serine and threonine residues, thereby impairing insulin signaling (Eldar-Finkelman and Krebs, 1997). In the present study, SREBP-1c mRNA levels were found to be induced over 2.5 fold in the 0.5 mg/kg/d PFDoA group (Fig. 5A). Hence, we hypothesized that inhibition of liver GSK3 by PFDoA led to an increase in the transcriptional levels of SREBP-1c, which further down-regulated the PI3K/Akt signaling pathway. The inhibition of GSK3 and elevation of SREBP-1c might play crucial roles in controlling glycogen storage in the rat liver following exposure to PFDoA for 110 days.

In addition, SREBP1 can regulate a wide array of genes involved in lipid biosynthesis, including genes involved in *de novo* lipogenesis (FASn, acetyl co-A carboxylase (ACC1)), glycerol-3-phosphate acyltransferase (GPAT), lipoprotein lipase (LPL)), SCD1, CD36, and phospholipid biosynthesis (phosphocholine cytidylyltransferase, CCT) (Hagen et al., 2010). Thus, we determined the mRNA levels of FASn, SCD1 and CD36 as well as the TG and TC content in rat livers following exposure to different doses of PFDoA. The results showed that the mRNA levels of SCD1 and CD36 were also significantly induced in both PFDoA-treated groups, while the levels of FASn mRNA decreased in the 0.5 mg/kg/d PFDoA group (Fig. 5A). Meanwhile, liver TG and TC increased significantly in the PFDoA-treated

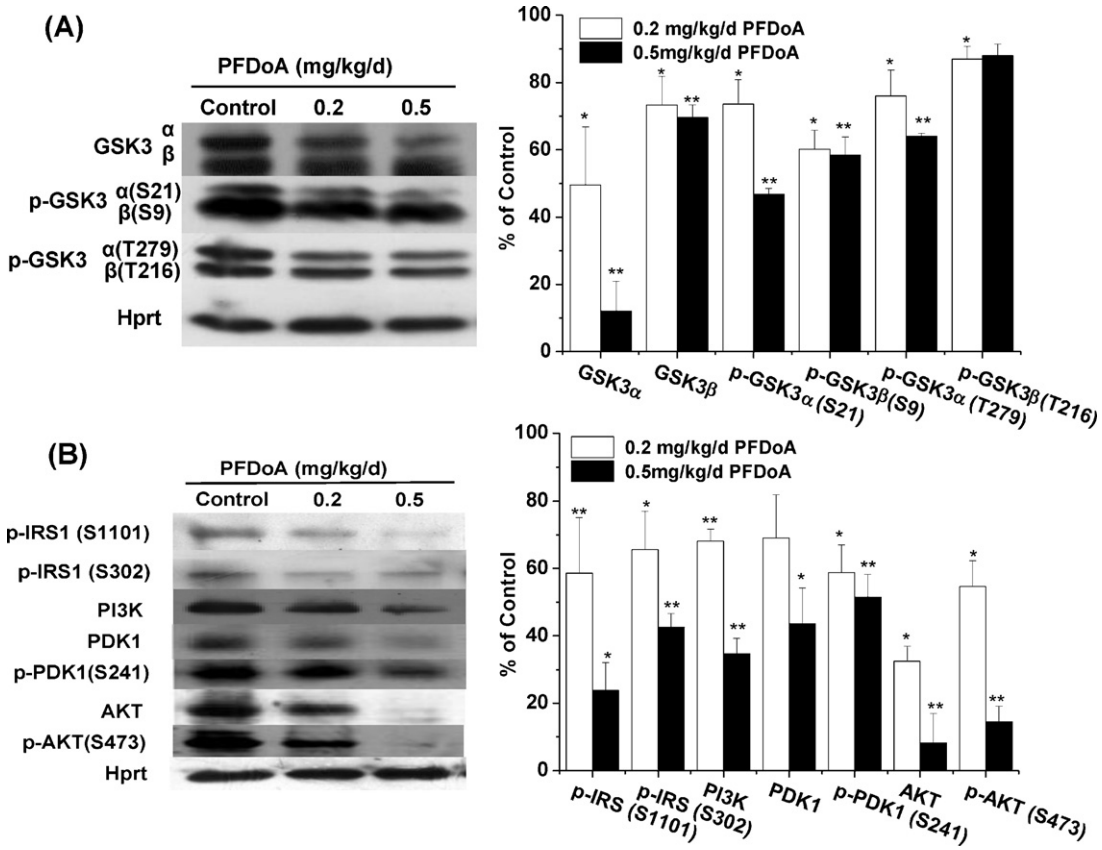

Fig. 4. Western blot analysis of protein levels in the rat liver following PFDoA exposure. (A) Western blot showing the levels of GSK3α/β proteins and phosphorylation (Tyr276/216 in GSK3α/β and Ser21/9 in GSK3α/β). (B) The phosphorylation levels of IRS1 (Ser1101 and Ser302), PDK1 (Ser241), and Akt (Ser473) and the protein levels of PDK1, Akt and PI3 kinase class III (PI3K) were measured. The left panel shows representative blots from three experiments. Hypoxanthine guanine phosphoribosyl transferase 1 (Hprt) was used as an internal control. The right panel shows the mean levels of protein bands compared to the control. Values indicate the mean ± SE of three rats per group, $^{*}p < 0.05$, $^{**}p < 0.01$.

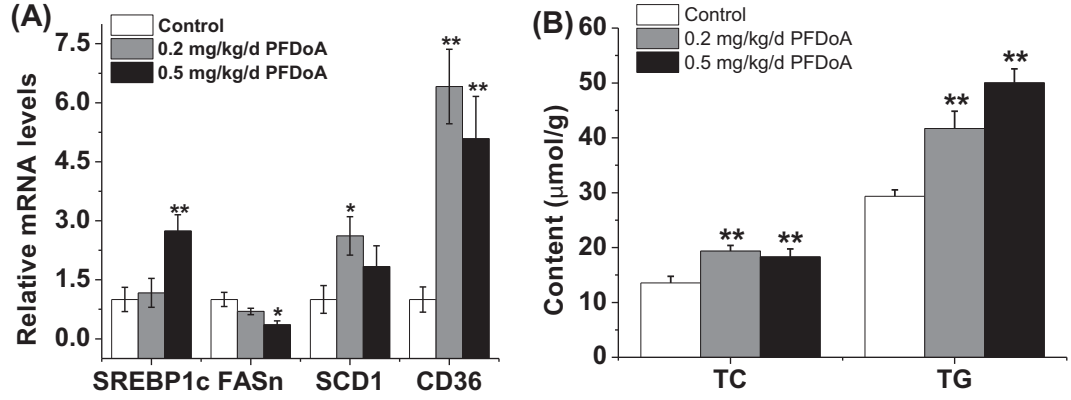

Fig. 5. Quantitative real-time PCR analysis of mRNA levels in the livers of control and PFDoA-exposed male rats. (A) mRNA levels of SREBP-1c, fatty acid synthase (FASn), SCD1 and fatty acid translocase (CD36), which are related to lipid storage. (B) Concentrations of triglyceride (TG) and total cholesterol (TC) in rat livers exposed to PFDoA for 110 days. Values indicate the mean ± SE of six rats per group, $^{*}p < 0.05$, $^{**}p < 0.01$.

groups (Fig. 5B). Thus, we speculated that long-term exposure to PFDoA could increase the lipid storage in the rat liver, mainly by inducing fatty acid transport to the liver, while the observed decrease in FASn mRNA levels might be due to negative feedback regulation of high lipid levels. Therefore, the inhibition of GSK3 and induction of SREBP-1c might contribute to metabolism related to lipid accumulation in the rat liver induced by chronic PFDoA exposure.

4. Conclusion

In this study, we identified a total of 1443 unique phosphopeptides from 769 phosphoproteins using high-sensitivity nano-electrospray and an LTQ-Orbitrap in control and PFDoA treated rat livers. Among these phosphorylation sites, 143 were identified as novel phosphorylation sites in 124 phosphoproteins. Signal pathway and network analysis revealed that GSK3 might

play a role in PFDoA-induced hepatotoxicity. Western blot and biochemical analysis further confirmed that the protein and phosphorylation levels of GSK3 were reduced following chronic PFDoA exposure. Also, several other proteins (IRS, PDK1 and Akt) in insulin signal pathway were reduced, which would cause insulin resistance-like changes and affect the lipid accumulation in the rat liver. However, the exact mechanism underlying this process requires further investigation. This report provides a more comprehensive view of phosphorylation networks related to the toxicities of persistent organic pollutants and could facilitate the discovery of new biomarkers for PFAAs toxicity. Future research into the functions of the identified novel phosphorylation sites will also be necessary.

Conflict of interest statement

The author declares that there are no conflicts of interest.

Acknowledgment

This work was supported by the National Key Basic Research Program of China (973 Program: 2013CB945204) and the National Natural Science Foundation of China (Grant No. 31025006).

Appendix A. Supplementary data

Supplementary data associated with this article can be found, in the online version, at http://dx.doi.org/10.1016/j.toxlet.2013.01.012.

References

Amanchy, R., Periaswamy, B., Mathivanan, S., Reddy, R., Tattikota, S.G., Pandey, A., 2007. A curated compendium of phosphorylation motifs. Nature Biotechnology 25, 285–286.

Beausoleil, S.A., Jedrychowski, M., Schwartz, D., Elias, J.E., Villen, J., Li, J., Cohn, M.A., Cantley, L.C., Gygi, S.P., 2004. Large-scale characterization of HeLa cell nuclear phosphoproteins. Proceedings of the National Academy of Sciences of the United States of America 101, 12130–12135.

Cross, D.A., Alessi, D.R., Cohen, P., Andjelkovich, M., Hemmings, B.A., 1995. Inhibition of glycogen synthase kinase-3 by insulin mediated by protein kinase B. Nature 378, 785–789.

Dai, J., Jin, W.H., Sheng, Q.H., Shieh, C.H., Wu, J.R., Zeng, R., 2007. Protein phosphorylation and expression profiling by Yin-yang multidimensional liquid chromatography (Yin-yang MDLC) mass spectrometry. Journal of Proteome Research 6, 250–262.

Ding, L., Hao, F., Shi, Z., Wang, Y., Zhang, H., Tang, H., Dai, J., 2009. Systems biological responses to chronic perfluorododecanoic acid exposure by integrated metabonomic and transcriptomic studies. Journal of Proteome Research 8, 2882–2891.

Eldar-Finkelman, H., Krebs, E.G., 1997. Phosphorylation of insulin receptor substrate 1 by glycogen synthase kinase 3 impairs insulin action. Proceedings of the National Academy of Sciences of the United States of America 94, 9660–9664.

Fang, X., Feng, Y., Shi, Z., Dai, J., 2009. Alterations of cytokines and MAPK signaling pathways are related to the immunotoxic effect of perfluorononanoic acid. Toxicological Sciences 108, 367–376.

Feng, Y., Shi, Z., Fang, X., Xu, M., Dai, J., 2009. Perfluorononanoic acid induces apoptosis involving the Fas death receptor signaling pathway in rat testis. Toxicology Letters 190, 224–230.

Ficarro, S.B., McCleland, M.L., Stukenberg, P.T., Burke, D.J., Ross, M.M., Shabanowitz, J., Hunt, D.F., White, F.M., 2002. Phosphoproteome analysis by mass spectrometry and its application to *Saccharomyces cerevisiae*. Nature Biotechnology 20, 301–305.

Frame, S., Cohen, P., Biondi, R.M., 2001. A common phosphate binding site explains the unique substrate specificity of GSK3 and its inactivation by phosphorylation. Molecular Cell 7, 1321–1327.

Gatzka, M., Walsh, C.M., 2007. Apoptotic signal transduction and T cell tolerance. Autoimmunity 40, 442–452.

Guruge, K.S., Taniyasu, S., Yamashita, N., Wijeratna, S., Mohotti, K.M., Seneviratne, H.R., Kannan, K., Yamanaka, N., Miyazaki, S., 2005. Perfluorinated organic compounds in human blood serum and seminal plasma: a study of urban and rural tea worker populations in Sri Lanka. Journal of Environmental Monitoring 7, 371–377.

Hagen, R.M., Rodriguez-Cuenca, S., Vidal-Puig, A., 2010. An allostatic control of membrane lipid composition by SREBP1. FEBS Letters 584, 2689–2698.

Hanahan, D., Weinberg, R.A., 2000. The hallmarks of cancer. Cell 100, 57–70.

Hers, I., Vincent, E.E., Tavare, J.M., 2011. Akt signalling in health and disease. Cellular Signalling 23, 1515–1527.

Houde, M., Martin, J.W., Letcher, R.J., Solomon, K.R., Muir, D.C., 2006. Biological monitoring of polyfluoroalkyl substances: a review. Environmental Science and Technology 40, 3463–3473.

Hughes, K., Nikolakaki, E., Plyte, S.E., Totty, N.F., Woodgett, J.R., 1993. Modulation of the glycogen synthase kinase-3 family by tyrosine phosphorylation. EMBO Journal 12, 803–808.

Jiang, X., Ye, M., Cheng, K., Zou, H., 2010. ArMone: a software suite specially designed for processing and analysis of phosphoproteome data. Journal of Proteome Research 9, 2743–2751.

Jones, P.D., Hu, W., De Coen, W., Newsted, J.L., Giesy, J.P., 2003. Binding of perfluorinated fatty acids to serum proteins. Environmental Toxicology and Chemistry 22, 2639–2649.

Kennedy Jr., G.L., Butenhoff, J.L., Olsen, G.W., O'Connor, J.C., Seacat, A.M., Perkins, R.G., Biegel, L.B., Murphy, S.R., Farrar, D.G., 2004. The toxicology of perfluorooctanoate. Critical Reviews in Toxicology 34, 351–384.

Kim, K.H., Song, M.J., Yoo, E.J., Choe, S.S., Park, S.D., Kim, J.B., 2004. Regulatory role of glycogen synthase kinase 3 for transcriptional activity of ADD1/SREBP1c. Journal of Biological Chemistry 279, 51999–52006.

. Kissa, E. (Ed.), 2001. Fluorinated Surfactants and Repellents, Marcel Dekker, New York.

Kudo, N., Suzuki-Nakajima, E., Mitsumoto, A., Kawashima, Y., 2006. Responses of the liver to perfluorinated fatty acids with different carbon chain length in male and female mice:in relation to induction of hepatomegaly, peroxisomal beta-oxidation and microsomal 1-acylglycerophosphocholine acyltransferase. Biological and Pharmaceutical Bulletin 29, 1952–1957.

Kweon, H.K., Hakansson, K., 2006. Selective zirconium dioxide-based enrichment of phosphorylated peptides for mass spectrometric analysis. Analytical Chemistry 78, 1743–1749.

Larsen, M.R., Thingholm, T.E., Jensen, O.N., Roepstorff, P., Jorgensen, T.J., 2005. Highly selective enrichment of phosphorylated peptides from peptide mixtures using titanium dioxide microcolumns. Molecular and Cellular Proteomics 4, 873–886.

Lau, C., Anitole, K., Hodes, C., Lai, D., Pfahles-Hutchens, A., Seed, J., 2007. Perfluoroalkyl acids: a review of monitoring and toxicological findings. Toxicological Sciences 99, 366–394.

Lau, C., Butenhoff, J.L., Rogers, J.M., 2004. The developmental toxicity of perfluoroalkyl acids and their derivatives. Toxicology and Applied Pharmacology 198, 231–241.

Linding, R., Jensen, L.J., Ostheimer, G.J., van Vugt, M.A., Jorgensen, C., Miron, I.M., Diella, F., Colwill, K., Taylor, L., Elder, K., Metalnikov, P., Nguyen, V., Pasculescu, A., Jin, J., Park, J.G., Samson, L.D., Woodgett, J.R., Russell, R.B., Bork, P., Yaffe, M.B., Pawson, T., 2007. Systematic discovery of in vivo phosphorylation networks. Cell 129, 1415–1426.

Liu, W., Xu, L., Li, X., Jin, Y.H., Sasaki, K., Saito, N., Sato, I., Tsuda, S., 2011. Human nails analysis as biomarker of exposure to perfluoroalkyl compounds. Environmental Science and Technology 45, 8144–8150.

Liu, Y., Wang, J., Wei, Y., Zhang, H., Xu, M., Dai, J., 2008. Induction of time-dependent oxidative stress and related transcriptional effects of perfluorododecanoic acid in zebrafish liver. Aquatic Toxicology 89, 242–250.

Martin, J.W., Whittle, D.M., Muir, D.C., Mabury, S.A., 2004. Perfluoroalkyl contaminants in a food web from Lake Ontario. Environmental Science and Technology 38, 5379–5385.

Moser, K., White, F.M., 2006. Phosphoproteomic analysis of rat liver by high capacity IMAC and LC–MS/MS. Journal of Proteome Research 5, 98–104.

Nagano, K., Shinkawa, T., Mutoh, H., Kondoh, O., Morimoto, S., Inomata, N., Ashihara, M., Ishii, N., Aoki, Y., Haramura, M., 2009. Phosphoproteomic analysis of distinct tumor cell lines in response to nocodazole treatment. Proteomics 9, 2861–2874.

Ohmori, K., Kudo, N., Katayama, K., Kawashima, Y., 2003. Comparison of the toxicokinetics between perfluorocarboxylic acids with different carbon chain length. Toxicology 184, 135–140.

Olsen, G.W., Ellefson, M.E., Mair, D.C., Church, T.R., Goldberg, C.L., Herron, R.M., Medhdizadehkashi, Z., Nobiletti, J.B., Rios, J.A., Reagen, W.K., Zobel, L.R., 2011. Analysis of a homologous series of perfluorocarboxylates from American Red Cross adult blood donors, 2000–2001 and 2006. Environmental Science and Technology 45, 8022–8029.

Olsen, J.V., Blagoev, B., Gnad, F., Macek, B., Kumar, C., Mortensen, P., Mann, M., 2006. Global, in vivo, and site-specific phosphorylation dynamics in signaling networks. Cell 127, 635–648.

Pan, Y., Shi, Y., Wang, J., Jin, X., Cai, Y., 2011. Pilot investigation of perfluorinated compounds in river water, sediment, soil and fish in Tianjin, China. Bulletin of Environment Contamination and Toxicology 87, 152–157.

Reiner, J.L., O'Connell, S.G., Moors, A.J., Kucklick, J.R., Becker, P.R., Keller, J.M., 2011. Spatial and temporal trends of perfluorinated compounds in Beluga Whales (*Delphinapterus leucas*) from Alaska. Environmental Science and Technology 45, 8129–8136.

Ros, S., Garcia-Rocha, M., Dominguez, J., Ferrer, J.C., Guinovart, J.J., 2009. Control of liver glycogen synthase activity and intracellular distribution by phosphorylation. Journal of Biological Chemistry 284, 6370–6378.

Rosen, M.B., Schmid, J.R., Corton, J.C., Zehr, R.D., Das, K.P., Abbott, B.D., Lau, C., 2010. Gene expression profiling in wild-type and PPARalpha-null mice exposed to perfluorooctane sulfonate reveals PPARalpha-independent effects. PPAR Research, http://dx.doi.org/10.1155/2010/794739.

Rush, J., Moritz, A., Lee, K.A., Guo, A., Goss, V.L., Spek, E.J., Zhang, H., Zha, X.M., Polakiewicz, R.D., Comb, M.J., 2005. Immunoaffinity profiling of tyrosine phosphorylation in cancer cells. Nature Biotechnology 23, 94–101.

Schwartz, D., Gygi, S.P., 2005. An iterative statistical approach to the identification of protein phosphorylation motifs from large-scale data sets. Nature Biotechnology 23, 1391–1398.
Shi, X., Yeung, L.W., Lam, P.K., Wu, R.S., Zhou, B., 2009. Protein profiles in zebrafish (*Danio rerio*) embryos exposed to perfluorooctane sulfonate. Toxicological Sciences 110, 334–340.
Stambolic, V., Woodgett, J.R., 1994. Mitogen inactivation of glycogen synthase kinase-3 beta in intact cells via serine 9 phosphorylation. Biochemical Journal 303 (Pt 3), 701–704.
Taniguchi, C.M., Emanuelli, B., Kahn, C.R., 2006. Critical nodes in signalling pathways: insights into insulin action. Nature Reviews Molecular Cell Biology 7, 85–96.
Villen, J., Beausoleil, S.A., Gerber, S.A., Gygi, S.P., 2007. Large-scale phosphorylation analysis of mouse liver. Proceedings of the National Academy of Sciences of the United States of America 104, 1488–1493.
Wei, Y., Chan, L.L., Wang, D., Zhang, H., Wang, J., Dai, J., 2008. Proteomic analysis of hepatic protein profiles in rare minnow (*Gobiocypris rarus*) exposed to perfluorooctanoic acid. Journal of Proteome Research 7, 1729–1739.
Woodgett, J.R., 1990. Molecular cloning and expression of glycogen synthase kinase-3/factor A. EMBO Journal 9, 2431–2438.
Wu, J., Shakey, Q., Liu, W., Schuller, A., Follettie, M.T., 2007. Global profiling of phosphopeptides by titania affinity enrichment. Journal of Proteome Research 6, 4684–4689.
Zhang, H., Ding, L., Fang, X., Shi, Z., Zhang, Y., Chen, H., Yan, X., Dai, J., 2011. Biological responses to perfluorododecanoic acid exposure in rat kidneys as determined by integrated proteomic and metabonomic studies. PLoS ONE 6, e20862.
Zhang, H., Shi, Z., Liu, Y., Wei, Y., Dai, J., 2008. Lipid homeostasis and oxidative stress in the liver of male rats exposed to perfluorododecanoic acid. Toxicology and Applied Pharmacology 227, 16–25.
Zhang, T., Sun, H.W., Wu, Q., Zhang, X.Z., Yun, S.H., Kannan, K., 2010. Perfluorochemicals in meat, eggs and indoor dust in China: assessment of sources and pathways of human exposure to perfluorochemicals. Environmental Science and Technology 44, 3572–3579.
Zolnierowicz, S., Bollen, M., 2000. Protein phosphorylation and protein phosphatases De Panne, Belgium, September 19–24, 1999. EMBO Journal 19, 483–488.